



Estimation of the Surface Stress from the Streamwise Pressure Gradient: The Kármán Integral Momentum Equation Revisited

P.A. FINDLATER^a, W.D. SCOTT^b, S.E. GREENHILL^b and J.M. HOPWOOD^c

^aDepartment of Agriculture, Western Australia, Geraldton, Western Australia 6531

^bMurdoch University, Murdoch, Western Australia 6150

^cUniversity of Western Australia, Crawley, Western Australia 6000

Received 12 September 2002; accepted in revised form 15 April 2004

Abstract. A method is developed to estimate the stress at the surface in a portable wind tunnel for wind erosion studies. The boundary layer height and the pressure gradient are used in a simple expression from the Kármán Integral Momentum Equation. Values of friction velocity u_* are within 10% of experimental values obtained through correlation techniques, including measurements of differential pressures with the Murdoch Turbulence Probe MTP and the X-wire, hot-wire anemometer XWA. Wind velocity and stress profiles reveal logarithmic trends and a 'constant stress layer' near the surface in the DAWA portable wind tunnel. Realignment of the statistics with the mean wind is essential.

Key words: agriculture, cross-wire, erosion, hot-wire, integral, Kármán, karman, momentum, Murdoch Turbulence Probe, shear, stress, wind tunnel

Abbreviations: DAWA – Department of Agriculture, Western Australia–formerly, West Australian Department of Agriculture and also Agriculture WA; MTP – Murdoch Turbulence Probe; XWA – X-Wire Anemometer, a cross-wire, hot-wire anemometer.

1. Introduction

A primary consideration in wind erosion studies is the measurement of the force of the wind on the surface. The wind must comply with the surface and, in shear, transfers momentum to the surface through turbulent eddies. The momentum transfer is exhibited as a mean stress, both in the wind and on the surface, the 'surface shear stress' τ_o . This stress moves particles and promotes erosion. An aim of the present paper and the paper of Findlater *et al.* [1] is a robust characterisation of surface shear stress, particularly for wind erosion studies. Ultimately, requirements for measurements in wind tunnels (in the field) and in the atmosphere (in the field) should evolve. Scaling considerations should allow measurements in prescribed wind environments, as produced by an agricultural wind tunnel, to be used in real, atmospheric erosion events over real and varying surfaces.

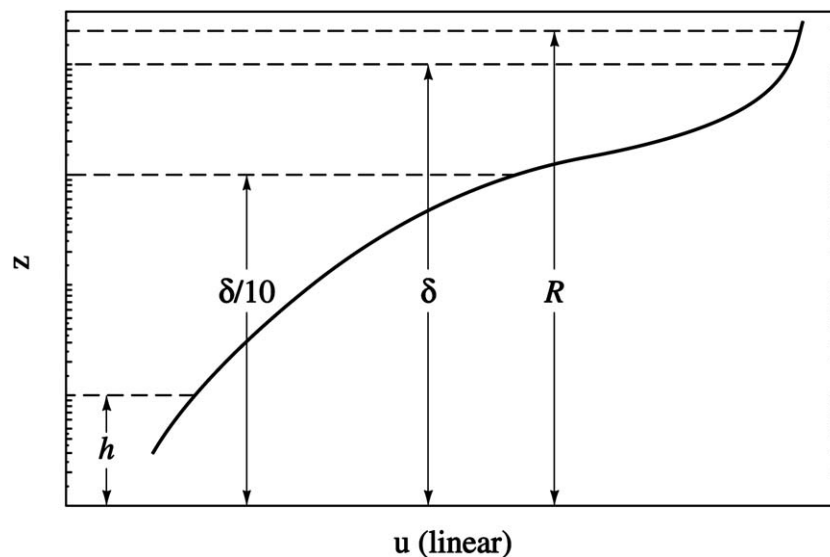


Figure 1. Schematic of a boundary layer flow. h , δ and R are the heights of the roughness elements, the boundary layer and the reference height in the freestream, respectively.

Techniques are available to estimate the surface stress τ_o in both the atmosphere and low speed wind tunnels: A drag plate measures τ_o directly. Pressure taps on roughness elements can give an indirect measurement (Antonia and Luxton [2, 3]). Cross-wire anemometers (XWA) can measure the Reynolds stress. The slope of the wind speed profile, the friction velocity u_* (m/s), may be an estimate of the stress.

These techniques have limitations: Considerable errors arise with drag plates from the turning moment when roughness elements are tall. Reynolds stress measurements assume that the fluid stress equals τ_o close to the surface. Determination of u_* from a velocity profile assumes that the flow is steady, in equilibrium and obeys the law of the wall. This may not be the case, particularly when fetches are short or there are changes in roughness. An alternative to these indirect methods but not commonly used, considers the Kármán Integral Momentum Equation.

Proposed by von Kármán [4], brief accounts of its potential are given in texts (Sutton [5]; Townsend [6]; Daily and Harleman [7]). It was successfully used by Marshall [8] to validate the use of drag plates in a wind tunnel study of roughness element geometry and spacing. The technique's principle advantages are: (1) it is conceptually sound; and (2) it can allow for non-steady and non-equilibrium flow.

This paper briefly rederives a general form of the Kármán Integral Momentum Equation, including error terms. The method for calculating τ_o is validated experimentally using correlation techniques with both the Murdoch Turbulence Probe (MTP) and the cross-wire anemometer (XWA).

The scene is presented in Figure 1; the streamwise wind u is plotted against the logarithm of the height z . The roughness elements on the surface have notional height h and scale the flow near the surface. Most variation in the wind occurs

within the boundary layer δ . The reference height R defines a central or freestream wind that varies little with height. The inner layer height is roughly $\frac{1}{10} \cdot \delta$, a region over which a logarithmic profile, ‘the law of the wall’, may apply. Close to δ an alternate logarithmic form, ‘the law of the wake’, may apply. Logarithmic forms may make up the entire velocity profile (see Bird *et al.* [9], p. 164). Nevertheless, Figure 1 is purposely presented so as not to suggest straight lines but a generalised profile; the Kármán derivation is not dependent on the presence or absence of straight lines or logarithmic features.

The following is a succinct derivation of the Karman Integral Momentum Equation (Equation (8)). In equilibrium, steady flow conditions this becomes nearly trivial (Equation (9)). The presentation, however, allows an estimate of the magnitude of the error in non-equilibrium flow conditions (Equation (10)). The approach is independent of the averaging technique or turbulence effects but this very brief derivation is for a turbulent boundary with all terms averaged appropriately in time – but the equations include no overbars on the dependent symbols. The flow is two-dimensional with a horizontal pressure gradient.

The variation of horizontal pressure gradient in the vertical is neglected. This is a classic, working assumption of most boundary layer models (see, for example, Schlichting and Gersten [10], Equation (6.9), p. 148). The boundary layer is considered a perturbation of the main flow near the boundary; the horizontal pressure gradient is manifest in the main flow and the pressure outside of the boundary layer is ‘impressed’ on the boundary layer.

2. The Momentum Integral Method

Attention is focused on the boundary layer, of height δ (see Schlichting and Gersten [10], p. 30). The derivation is a composite of the approaches of Townsend, Marshall, Daily and Harleman, and Sutton. The objective is a simple, working form of the Kármán’s Integral Momentum Equation from which the surface stress τ_o may be obtained, and an estimate of the error. Consider the time-averaged, streamwise Navier–Stokes Equation for two-dimensional flow,

$$\frac{\partial u}{\partial t} + u \frac{\partial u}{\partial x} + w \frac{\partial u}{\partial z} = -\frac{1}{\rho} \frac{\partial p}{\partial x} + \frac{1}{\rho} \frac{\partial \tau}{\partial z}, \quad (1)$$

where the normal stress is absorbed in p ; the turbulence is isotropic or small in intensity (Carminati *et al.* [11]). The equation is otherwise valid for either laminar or turbulent flow of a fluid of constant density ρ . However, with the dominance of turbulence in the atmosphere and our wind tunnel, we note that the shear stress τ is logically treated as the time averaged Reynold’s stress,

$$\tau = -\rho \overline{u'w'} = \rho u_*^2, \quad (2)$$

the stress in the fluid directed along the main flow on a plane perpendicular to the vertical. Note that this generalised definition for u_* only predicts τ_o under restricted

conditions; in steady and equilibrium flow, close to the ground, within a logarithmic or constant stress layer.

For a steady state (1) becomes

$$\frac{\partial(u^2)}{\partial x} + \frac{\partial(uw)}{\partial z} = -\frac{1}{\rho} \frac{\partial p}{\partial x} + \frac{1}{\rho} \frac{\partial \tau}{\partial z} \quad (3)$$

with the use of the chain rule and the continuity equation,

$$\frac{\partial u}{\partial x} + \frac{\partial w}{\partial z} = 0. \quad (4)$$

Integrate the entire Equation (3) over δ .

$$\int_0^\delta \frac{\partial(u^2)}{\partial x} dz + \int_0^\delta \frac{\partial(uw)}{\partial z} dz = -\frac{1}{\rho} \int_0^\delta \frac{\partial p}{\partial x} dz + \frac{1}{\rho} \int_0^\delta \frac{\partial \tau}{\partial z} dz. \quad (5)$$

This is the basic equation of the integral method; all the terms can be simplified. Provided u^2 is a well-behaved function, the operations of integration and differentiation can be interchanged¹ in the first term. The second term is simply the product uw evaluated between the two limits and $u_0 w_0$ must be zero at the wall. The pressure gradient $\frac{\partial p}{\partial x}$ is assumed not to be a function of z so the term becomes simply the gradient multiplied by δ . The last term is $-\tau_0/\rho$ since τ must be close to zero near the main stream. Hence we have

$$\frac{\partial}{\partial x} \int_0^\delta u^2 dz - u_\delta^2 \frac{\partial \delta}{\partial x} + u_\delta w_\delta = -\frac{\delta}{\rho} \frac{\partial p}{\partial x} - \frac{\tau_0}{\rho}. \quad (6)$$

Now, from (4), knowing $w_0 = 0$

$$w_\delta = -\int_0^\delta \frac{\partial u}{\partial x} dz = -\frac{\partial}{\partial x} \int_0^\delta u dz + u_\delta \frac{\partial \delta}{\partial x}. \quad (7)$$

The steady Boundary Integral Equation is therefore

$$\frac{\tau_0}{\rho} = -\frac{\delta}{\rho} \frac{\partial p}{\partial x} + u_\delta \frac{\partial}{\partial x} \int_0^\delta u dz - \frac{\partial}{\partial x} \int_0^\delta u^2 dz. \quad (8)$$

This equation suits the present purposes, and allows an estimate of error. Clearly, if the profile is unchanging or 'in equilibrium'

$$\frac{\tau_0}{\rho} \cong -\frac{\delta}{\rho} \frac{\partial p}{\partial x} \quad (9)$$

an equation easily obtained² from (1) and expected in channels in equilibrium flow (see Tennekes and Lumley [12], Equation (5.2.5)). The advantage with this

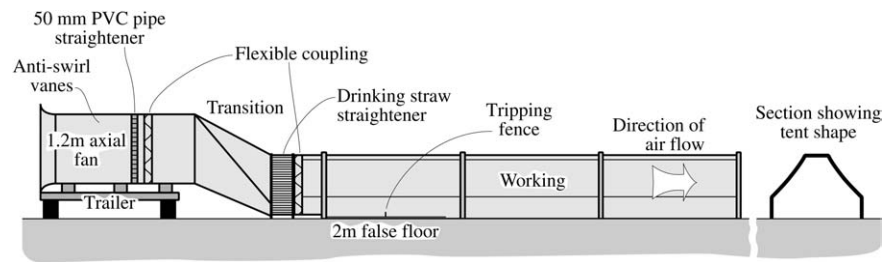


Figure 2. Wind tunnel design of agriculture Western Australia.

approach, using Equation (8), is that the effect of non-equilibrium flow can be estimated.

The conditions imposed are:

- (1) Two-dimensional flow with small or isotropic turbulence
- (2) Steady, well-behaved flow and
- (3) An equilibrium profile.

This simple result (9) states that the surface stress τ_o is equal to the product of the boundary height and the pressure gradient.

3. Method and Instrumentation

Estimates of the surface stress from the Kármán expression (9) were compared with XWA measurements and also measurements from the Murdoch Turbulence Probe (MTP) (see Section 5). Comparisons in terms of u_* values are in Figure 7. The boundary layer height δ in (9) was determined from abrupt changes in the wind speed profile, as well as profiles of the integral length scale Λ . Antonia and Luxton [2, 3] suggest that the height of the internal boundary layer resulting from a change in surface roughness can be defined by the intersection of the profiles above and below a knee, with the profile plotted as a function of z (see Figure 4). The pressure gradient $\frac{\partial p}{\partial x}$ was measured using two pressure taps flush with the ceiling of the tunnel 3.08 m apart; the pressure difference was measured with the MTP by removing the head and using tubing.

4. The DAWA Tunnel

The portable wind tunnel developed for wind erosion research by the Department of Agriculture, Western Australia (DAWA), Figure 2, was modified from that used by Findlater *et al.* [13], retaining its tent-shaped design. It is driven by a single stage 1.2 m axial fan and a diesel engine, mounted on a trailer. The flow from the fan passes through a honeycomb straightener of PVC tubing 56 mm in diameter, 130 mm long. From there, the flow is diverted down to ground level through a short transition partitioned into 4 sections with internal vanes of equal cross sectional area (designed by Brancatisano and Trinh [14]). The flow then passes through

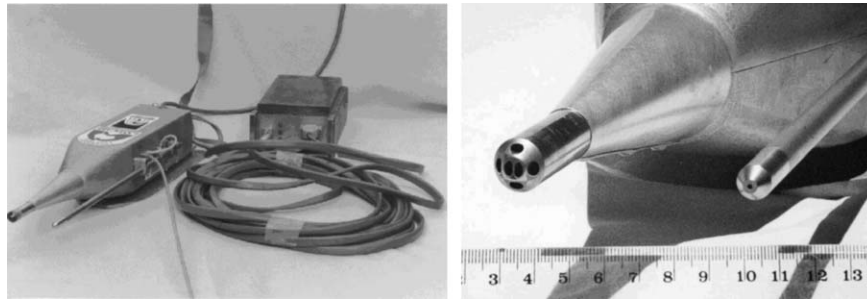


Figure 3. Turbulence Probe used to measure the velocity components, Reynolds stresses, integral length scale and turbulence intensity.

a second honeycomb composed of drinking straws into a 7.1 m horizontal duct. About 1 m further along a 40 mm high tripping fence hastens the development of equilibrium flow. The fence is located midway on a 2 m false floor to prevent scouring. The working section has a total length of 5.1 m and an area for flow of about 1 m²; the tent-shape maximises the exposure of bare ground in the working section.

Measurements are reported over a 'standard' surface constructed of cylinders (see Findlater *et al.* [1], and Raupach *et al.* [15], surface E), and a 'smooth' bitumen surface. Velocity profiles were measured with a rake of pitot and static tubes coupled to a multi-tube inclined manometer (Findlater *et al.* [1]). Measurements of turbulence, Reynolds stresses and integral scales were made using correlation techniques, taking advantage of Fourier Transform Techniques with the Murdoch Turbulence Probe (Figure 3). Occasional companion measurements were made with a XWA.

During erosion studies the flow is controlled by engine speed. The speed is initially 800 rpm, below the threshold for erosion. Each minute the speed is increased by 200 rpm up to 2200 rpm. In the present work the engine speed was held constant until the measurements were completed.

5. Murdoch Turbulence Probe MTP

The MTP (Figure 3) was developed³ at Murdoch University for the National Soil Conservation Programme and the Land and Water Resources, Research and Development Corporation (see Smith [16]; Scott *et al.* [17]). The Probe is held rigid and level on a heavy steel plate aligned with the longitudinal axis of the wind tunnel. The pitot-static head is a 15 mm diameter truncated cone of a CETIAT design; 6 pressure ports of 2 to 3 mm sense differential pressures that are converted into the three components of velocity. (See Findlater *et al.* [1], p. 11, Smith [16] or Findlater [18], for details.)

The data are processed in nearly real time. The stresses and spectra are based on correlations between the instantaneous streamwise, lateral and vertical wind

Table I. Correlation (r) between Probe with a five port spherical head, and cross-wire measurements Smith [16])

Mean velocity	0.996
Reynolds stress	0.962
Integral time scale	0.920
Integral length scale	0.710

speeds. Fourier transform techniques are used to correct for attenuation and phase lags; the correlations and average winds are calculated and a matrix transformation aligns the statistics with the mean wind; turbulence spectra and integral scales are calculated. The Integral Length Scale Λ is defined for the streamwise wind, using time averaging and Taylor's hypothesis (see Findlater *et al.* [1], p. 10). A pitot-static tube of CETIAT design mounted alongside the probe acts as a reference (see Figure 3b, right side).

An early design of the MTP (with a spherical head) was calibrated in a laminar flow tunnel and tested against a cross-wire in the DAWA tunnel by Smith [16]. The correlations (r) between the probe and the hot wire over the 'standard' test surface are presented in Table I. The present CETIAT design (Figure 3) proved superior to the spherical head; the CETIAT design retained the properties of the spherical head with a cross-flow angle greater than 50° (Smith [16]).

6. Results and Discussion

Using the method described by Antonia and Luxton [2, 3], velocity profiles normalised by a reference height of $R = 0.512$ m were plotted over a range of flow rates (Figure 4). The data were collected near the downstream end of the DAWA wind tunnel with engine speeds ranging from 1000 to 2200 rpm. With normalization all the data can be fitted to a single profile. Three sets of regression lines can be drawn through the profile, producing two knees. Complementary sets of measurements on page 375 show the Reynolds stresses (Figure 5); the stresses are constant up to about 0.1 m and increase to about zero at 0.4 m; the Integral Length Scale Λ (Figure 6) is constant to about 0.3 m. We suggest the lower knee at about $(0.3)^2 \sim 0.1$ m corresponds to the top of the 'constant stress layer', and the second knee at about $(0.55)^2 \sim 0.3$ m defines the top of the boundary layer δ (see Figure 1).

The 'constant stress layer' is clearly identified in Figure 5 and is a classical feature in many laboratory and field experiments. Raupach *et al.* [15] studied arrays of rough surfaces and report regions of constant stress up to about 30% of the boundary layer. In agricultural designs with similar roughnesses, (Raupach and Leys [19], Figure 8) show similar regions of constant stress. It '*occurs close to the walls in most turbulent boundary layers*' (Tennekes and Lumley [12], p. 54, line 3). The classic work of Bagnold [20] presents both laboratory and field measurements

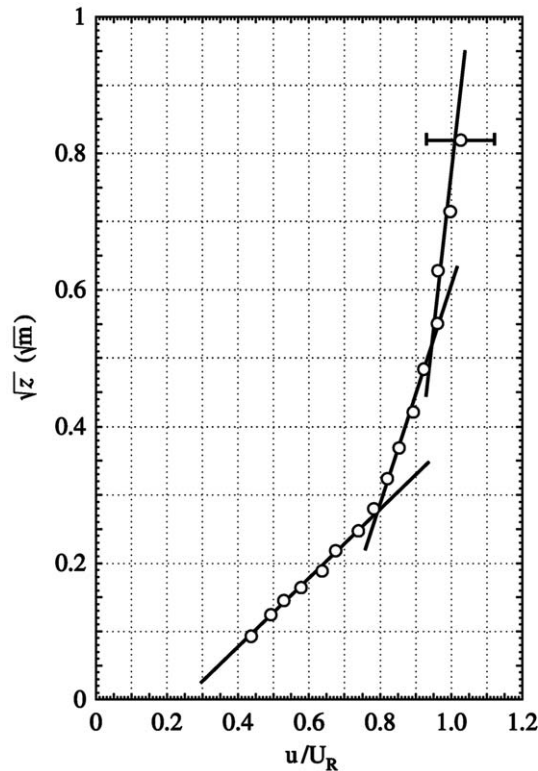


Figure 4. The profile of horizontal velocities, normalised to reference height R , 0.512 m, roughly the centre of the wind tunnel, for engine speeds of 1000 to 2200 rpm. Significant changes in the boundary layer are represented by the intersection of two lines, the 'knees' (Antonio and Luxton [2, 3]). The boundary layer height δ is considered to occur at the 'knee' around $z = 0.3$ m. Windspeeds U_R at $R = 0.512$ m used to normalise the data:

rpm	1000	1200	1400	1600	1800	2000	2200
m/s	8.15	9.95	11.72	13.37	15.12	16.84	18.60

based on the concept of a layer with a 'constant stress', a 'scaling velocity u_* ' or a 'logarithmic layer'. (Lyons and Scott [21], pp. 45–52) use the observation of a nearly constant stress to derive the logarithmic profile. It is arguable that the stress is truly constant in Figure 5 or in any 2D or 3D boundary layer; nevertheless these experimental measurements present a region of constant stress, somewhere below about 0.1 m.

Three independent techniques for estimating τ_o and u_* are compared in Figure 7, for the range of windspeeds: (1) Kármán integral momentum method with $\delta = 0.3$ m, (2) XWA, and (3) the MTP. The MTP values are shown on the abscissa; the correspondence between the MTP and the integral momentum values is presented as a series of open squares and a linear regression line passing through zero. The line would ideally have a slope of 1.00 but has a slope of 1.02. The circles

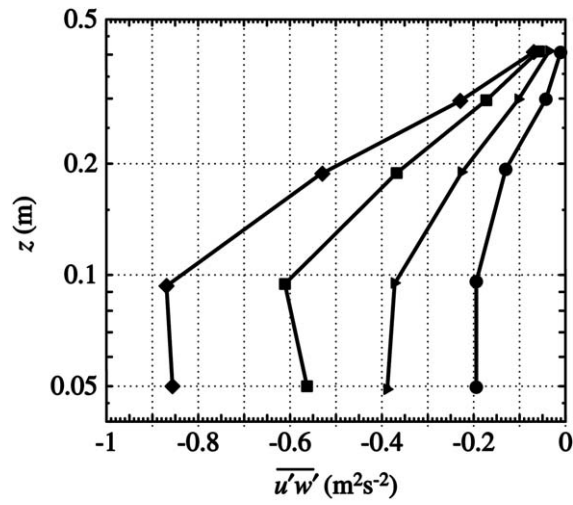


Figure 5. Reynolds stress profiles over a range of flow rates with engine speeds of 2200 (◆), 1800 (■), 1400 (▸), and 1000 (●) rpm.

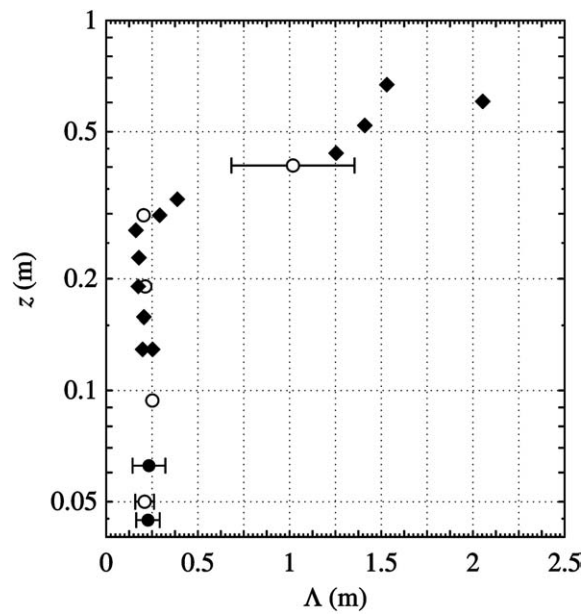


Figure 6. Variation of the Integral Length Scale Λ with height and windspeed.
 ◆ - Standard surface at engine speed of 1600 rpm.
 ○ - Standard surface at engine speeds of 1000, 1400, 1800 2200 rpm.
 ● - Bitumen surface at 1000, 1400 1800 and 2200 rpm.

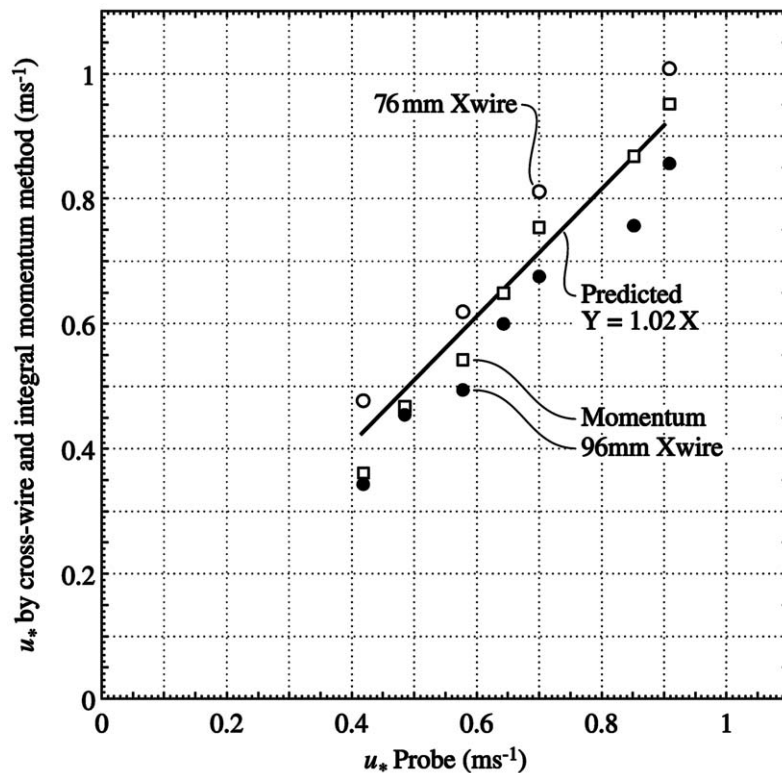


Figure 7. Comparison of friction velocity values obtained by the integral momentum method and measurements using a X-wire ($z = 76$ mm, $z = 95$ mm), with the Murdoch Turbulence Probe (Smith [16]).

represent XWA measurements of u_* at two heights, 76 mm and 95 mm. The MTP was placed 50 mm above the surface.

The XWA values measured at heights above the MTP may be 10% larger or 10% smaller than the MTP values. The XWA measurements are uncertain because the two hot wires do not measure the lateral wind; they drift, are difficult to maintain and position accurately and don't respond properly at large angles to the wind. The Murdoch Turbulence Probe is specially designed to make 3D measurements in harsh environments and minimise other effects. It measures differential pressures and is isolated from the environment but still does show a drift, with a time factor of about a month.

Scott [22] presents the method of *a posteriori* realignment of the statistics as used by the MTP processor. Correlation statistics and mean values are required for each wind component. The realignment could not be applied to the XWA. Scott⁴ has estimated the error involved using data from a high resolution 3-vane Gil Anemometer set (in the atmosphere) and the MTP (present data from the DAWA wind tunnel). It seems a $2\frac{1}{2}^\circ$ error in the vertical direction can produce a 20% error

in the shear stress and a 10% error in u_* . Ignorance of the lateral wind produces a small error provided the lateral wind is small compared to the longitudinal wind.

An alternate comparison can also be made using the wind profile. Most profiles in the DAWA wind tunnel are logarithmic, even well above the ‘boundary layer’ or ‘inner layer’. In different experiments, Findlater *et al.* ([1], see Figure 8 and Tables II and III) present profiles from a pitot rake and the MTP statistics. The u_* values from the slope of the profile and τ_o or Reynolds stresses $(\overline{u'w'})$ near the surface were used to estimate values of von Kármán’s constant κ . Four values measured in the same tunnel with surface roughnesses similar to the peg-board and similar windspeeds suggest that κ is around 0.3. Though the normally accepted value for atmospheric turbulence is 0.4, the lower value of 0.3 seems correct for estimating shear stresses from profiles in these agricultural wind tunnels (with ‘tripping fences’). One interpretation is that the logarithmic profile is more of a ‘law of the wake’ that scales from the top of the boundary layer. Using 0.4 rather than 0.3 (mistakenly, from the preceding argument) suggests the u_* estimates from the profile (outside $\delta/10$) would be 25% higher than values measured with the MTP (inside $\delta/10$).

The overall interpretation is that the MTP and XWA data on Figure 7 represent the same ‘constant stress values’ within a 10% error. They have a slope similar to the given line and straddle the u_* values calculated using the integral momentum method. We accept that the measured values are below about 0.1 m and expect that both the XWA and the MTP are measuring, roughly, the same values, in the ‘constant stress layer’.

7. Error Estimates

The Karman Integral Expression also allows an estimate of the error in measuring the shear stress in the wind tunnel, from the non-equilibrium development of the wind profile along the working section. The effect is approximated by the two right terms in equation 8. Two classical velocity profiles are considered; a separable, product solution and a logarithmic solution:

$$error = u_\delta \frac{\partial}{\partial x} \int_o^\delta u dz - \frac{\partial}{\partial x} \int_o^\delta u^2 dz. \quad (10)$$

7.1. SEPARABLE SOLUTION

A simple, general form for the profile might be

$$u(x, z) \approx F(x) \cdot G(z).$$

Substituting the above into Equation (10), noting that $\delta = \delta(x)$, and completing the differentiation with respect to x gives

$$\left(\frac{d}{dx}F(x)\right)\left(u_\delta \int_0^{\delta(x)} G(z)dz - 2F(x) \int_0^{\delta(x)} (G(z))^2 dz\right). \quad (11)$$

The DAWA wind tunnel has a wind profile that tends to be logarithmic⁵ so that $G(z) \approx \ln(\frac{z}{z_o})$. Inserting this logarithmic form into the error expression and integrating from $z = z_o$ to $z = \delta(x)$ gives an error of

$$\delta \left(\frac{d}{dx}F(x)\right)\left(3u_\delta - u_\delta \ln\left(\frac{\delta}{z_o}\right) - 4F(x)\right), \quad (12)$$

providing the vertical integration begins when $u = 0$ at roughness height z_o .

Information for assessment of this error includes upwind measurements; practically, however, placement of instruments upwind changes the conditions in the tunnel. The total flow through the tunnel must be preserved, however; provided some symmetry is maintained during the flow development, mass continuity dictates that⁶

$$\int_{z_o}^R u(x, z)dz = \int_{z_o}^R F(x) \ln\left(\frac{z}{z_o}\right)dz = \text{'a constant'}$$
 (13)

or

$$\text{'a constant'} = F(x) \left(R \ln\left(\frac{R}{z_o}\right) - R + z_o\right)$$

which means that $F(x)$ must be a constant, $\frac{d}{dx}F(x) = 0$, and from (11)

$$\text{error} \approx 0. \quad (14)$$

A product functional form for u , two separate functions of x and z , dictates that the flow must act as if at equilibrium.

7.2. LOGARITHMIC SOLUTION

Revealing is an alternate, logarithmic form with $z_o = g(x)$, 'roughness varying along the tunnel', with a composited form for the error,

$$\text{error} = \int_{g(x)}^{\delta(x)} \left(u_\delta \frac{\partial}{\partial x} u(x, z) - \frac{\partial}{\partial x} u(x, z)^2\right) dz. \quad (15)$$

The form $u(x, z) = f(x) \ln(\frac{z}{g(x)})$ is substituted; the error estimate is

$$\begin{aligned} &[-\Delta \ln^2(\Delta) + \ln(\Delta) + 3\Delta \ln(\Delta) - 4\Delta + 4] \cdot \frac{\partial}{\partial x} f(x) g(x) f(x) \\ &+ [\Delta \ln(\Delta) + \ln(\Delta) - 2\Delta + 2] \cdot \frac{\partial}{\partial x} g(x) f(x) f(x), \end{aligned} \quad (16)$$

where $\Delta = \frac{\delta(x)}{g(x)}$ is the height of the boundary layer measured in roughness lengths. Combine the terms containing Δ .

$$K \left(\frac{\partial}{\partial x} f(x) \right) g(x) f(x) + L \left(\frac{\partial}{\partial x} g(x) \right) f(x)^2, \tag{17}$$

K and L in Equation (17), would be constants if the relative boundary layer height Δ is constant; the velocity profile is ‘similar’ down the tunnel.

The coupling between the $f(x)$ and $g(x)$ is crucial to the estimate; as above, this is found using the continuity relationship:

$$\int_{g(x)}^R f(x) \ln\left(\frac{z}{g(x)}\right) dz = f(x) R \ln\left(\frac{R}{g(x)}\right) - f(x) R + f(x) g(x) = \text{const}, \tag{18}$$

which reveals that $f(x)$ and $\frac{\partial}{\partial x} f(x)$ are functions of $g(x)$.

$$f(x) = \frac{\text{const}}{g(x) + R \ln\left(\frac{R}{g(x)}\right) - R}, \tag{19}$$

$$\frac{\partial}{\partial x} f(x) := -\frac{\text{const} \left(\frac{\partial}{\partial x} g(x) \right) (-R + g(x))}{\left(g(x) + R \ln\left(\frac{R}{g(x)}\right) - R \right)^2 g(x)}. \tag{20}$$

Combining these results with equation 17 gives another estimate for the error.

$$\frac{\left(\frac{\partial}{\partial x} g(x) \right) \text{const}^2 (R - g(x)) K}{\left(g(x) + R \ln\left(\frac{R}{g(x)}\right) - R \right)^3} + \frac{\left(\frac{\partial}{\partial x} g(x) \right) \text{const}^2 L}{\left(g(x) + R \ln\left(\frac{R}{g(x)}\right) - R \right)^2}. \tag{21}$$

It is clear that $g(x)$ must vary with x for there to be an error. The reference height R is large compared to $g(x)$ and $R/g(x) \approx \Delta$. The coefficients of K and L are both positive so that the L term is always positive and the K term is always negative. A further, approximate form for the error is

$$\approx \frac{\frac{\partial}{\partial x} g(x) \left(\frac{\text{const}}{R} \right)^2}{(\ln(\Delta) - 1)^2} \left(\frac{K}{(\ln(\Delta) - 1)} + L \right) \tag{22}$$

or, substituting for K and L ,

$$\text{error} \approx \frac{\frac{\partial}{\partial x} g(x) \left(\frac{\text{const}}{\Delta g(x)} \right)^2}{(\ln(\Delta) - 1)^2} \left(\frac{\ln^2(\Delta) - 2\Delta + 4}{(\ln(\Delta) - 1)} - 2 \right). \tag{23}$$

This estimation suggests an error⁷ of around 10%, an error similar to that suggested on Figure 7. Importantly, evoking of mass continuity relates $f(x)$ and $g(x)$; K and L have opposite signs and there is a tendency for error cancellation. Both forms for the error; an arbitrary, separable product solution and a logarithmic solution, commonly presumed mean velocity profiles, lead to relatively small errors.

It seems clear that the error in estimating shear stress with the Kármán Integral method is small in the non-equilibrium flow of the DAWA wind tunnel.

The data (Figure 7) and above estimates bring the realisation that the error in using the Kármán Integral Method may be small or zero in non-equilibrium flow. Remarkable is the observation of a near-logarithmic velocity profile throughout this tunnel (Findlater *et al.* [1] and Raupach and Leys [19]). The logarithmic law seems to have some inherent merit itself; it is commonly observed in real flows (Lyons and Scott [21]), though it is a mistake to presume the logarithmic pattern is unique (Carminati *et al.* [11]). We conclude that shear stress can be measured with the Kármán Integral Momentum Method, even when the profile is out-of equilibrium. Shear stress data from two independent experimental methods confirm this.

The Kármán Integral Momentum Method is robust and calculation of shear stress is not dependent on having a boundary layer in a 'nearly equilibrium' state. Indeed, measuring τ_o and the pressure gradient can give a length scale, the boundary layer height δ . Small changes in the boundary layer are unlikely to correspond with large changes in the stress. The nature of the integral and the subtraction of similar terms tends toward minimization and cancellation of errors (see Equations (10) and (15)). Regardless of the theory, however, the effect is experimentally confirmed. Additionally, long woollen threads placed near the upper edge of the boundary layer revealed almost no drop along the length of the tunnel; variations were less than 10 cm⁸.

Acceptance of the technique and the data allows some speculation regarding scaling of the portable wind tunnel data and atmospheric data/effects. Integral scales were calculated for the longitudinal winds (see Figure 6). These scales may represent the average eddy size for 'frozen' turbulence along the wind direction. Within the boundary layer (with delta around 0.3 m), Λ is about 0.2 m; outside the boundary layer Λ is about 1.5 m. Little data on Lambda has been acquired with wind erosion (except the preliminary data presented by Findlater *et al.* [1] but it might be suggested that Λ scales the erosion, from the outer flow (1.5 m) to the inner flow (0.2 m). In an open atmospheric event, one expects the outer scale to be 10 m or more. Perhaps outer or inner values of Λ (or both) will give an appropriate length scale to the erosion, and allow credible application of data collected in the field to what is expected in the atmosphere.

8. Conclusions

The principal results of this research are:

- (1) In wind tunnels with pressure gradients and steady boundary layer flows, the surface stress can be determined from the product of the boundary layer height and the pressure gradient. The flow does not need to be in equilibrium.
- (2) The calculation uses the von Kármán Integral Momentum Equation and allows error estimates. Corroboration comes from three different experimental techniques: a cross-wire, hot-wire XWA; a pressure-based probe for measurements

in harsh flows, the Murdoch Turbulence Probe MTP; and wind profiles from a pitot rake.

- (3) The DAWA agricultural wind tunnel with a rough surface, turbulent eroding winds, a ‘tripping’ fence and a ‘well-developed flow’ has a logarithmic profile and a ‘constant stress layer’ near the surface.

Importantly, this experimental corroboration not only allows an analysis of non-equilibrium flows and estimation of u_* from the measured pressure gradient and the wind profile, but does so without the necessity of expensive and invasive equipment. That is, it is difficult to measure wind speeds in three directions, let alone during a sand blast; sensors and instruments placed in the flow or on the surface must alter the flow and/or disrupt the surface. Mean wind profiles combined with pressure gradient measurements can estimate surface shear stresses indirectly.

Notes

1. Unconsidered in the classical integral method is the term relating to the change in the boundary layer with x . The exact expression is

$$\int_0^\delta \frac{\partial(u^2)}{\partial x} dz = \frac{\partial}{\partial x} \int_0^\delta (u^2) dz - u_\delta^2 \frac{\partial \delta}{\partial x}.$$

The last term ‘cancels out’ in Equation (8).

2. If all the terms on the left side of (1) are ignored

$$\frac{\partial \tau}{\partial z} \cong \frac{\partial p}{\partial x} \Rightarrow \tau = \frac{\partial p}{\partial x} (z - \delta) \Rightarrow \tau_o = -\delta \frac{\partial p}{\partial x}.$$

3. Manufacturer: Roger Handsworth of Platypus Engineering, Hobart, Tasmania.
4. <http://maple.murdoch.edu.au/view.html#lateral>
5. Raupach and Leys [19], Figure 4, present data from a tunnel with a ‘tent-shape’ manufactured to the same plan as the present tunnel; all of our profile studies, including data from the same tunnel collected by the authors Findlater *et al.* [1], Figure 8, are nearly logarithmic. Apart from this, this calculation is independent of the functional form for $G(z)$, and a power function produces the same result.
6. A condition strictly adhered to in a pipe in non-compressible flow. The tent-shaped tunnel has different roughnesses on the lower and upper surfaces.
7. Associated values might be: $\Delta \approx 300$, $g(x) \approx .001 \text{ m}$, $g'(x) \approx 0.0001$, $\delta \approx 30 \text{ cm}$, $z_o \approx 1 \text{ mm}$ (see Findlater *et al.* [1]). Notionally the $g'(x)$ allows for a change in roughness of 10% in one meter of flow, along the tunnel. The *const* is the flow rate per lateral meter of tunnel which is around $5 \frac{\text{m}}{\text{s}}$. The shear stress values would be about $-0.6 \frac{\text{m}^2}{\text{s}^2}$ (see Figure 7, $u_* \approx 0.8$).
8. A thread must ‘slump’ along the tunnel. The lift or drag coefficients are mostly constant. As the thread ‘slumps’, it exposes more area to the flow and experiences more drag and lift. The ‘slumping’ also means falling toward the floor of the tunnel, where there is less wind and less drag and lift. The woolen thread attains a limited ‘holding position’ with a slope around 0.01 to 0.001 in a $10 \frac{\text{m}}{\text{s}}$ wind.

Acknowledgements

Support from DAWA is acknowledged, particularly from Dan Carter and Rob Hetherington, in Albany. John Tubb and Gibb Moore of Curtin University, Mechanical Engineering, were prime contributors to the research; unfortunately, Gibb passed away on 2 March 96. The advice of Michael R. Raupach and Yaping Shao from the CSIRO, Centre for Environmental Mechanics, contributed to the development and completion of this project. The major support was from the Australian National Soils Conservation programme and the Land and Water Resources Research and Development Corporation, under grant UMU5.

References

1. Findlater, P.A., Greenhill, S.E., and W.D. Scott: 2001, Design and testing of a turbulence probe for harsh flows, *J. Environ. Fluid Mech.*, **1**, March.
2. Antonia, R.A. and Luxton, R.E.: 1971, The response of the turbulent boundary layer to a step change in surface roughness. Part 1. Smooth-to-rough, *J. Fluid Mech.* **48**, 721–761.
3. Antonia, R.A. and Luxton, R.E.: 1972, The response of the turbulent boundary layer to a step change in surface roughness. Part 2. Rough-to-smooth, *J. Fluid Mech.* **53**, 737–757.
4. von Kármán, Th.: 1921, Über laminare und turbulente Reibung (About laminar and turbulent friction), *ZAMM (Zeitschrift für angewandte Mathematik und Mechanik)* **1**, 233–253. English translation in NACA (National Advisory Committee for Aeronautics, now NASA) Technical Memorandum TM 1092 ; see also *Collected Works II*, 70–97, London 1956; from Schlichting, *Ibid.*, pp. 159 and 162.
5. Sutton, O.E.: 1953, *Micrometeorology*, Kreiger, FL, 33 pp.
6. Townsend, A.A.: 1956, *The Structure of Turbulent Shear Flow*, Cambridge University Press, Cambridge, 315 pp.
7. Daily, J.W and Harleman, D.R.F.: 1966, *Fluid Dynamics*, MA, Addison-Wesley Publishing Company, Reading, MA, 454 pp.
8. Marshall, J.K.: 1971, Drag measurements in roughness arrays of varying density and distribution, *Agric. Meteorol.* **8**, 269–292.
9. Bird, R.B., Stewart, W.E. and Lightfoot, E.N.: 1960, *Transport Phenomena*, John Wiley, 780 pp.
10. Schlichting, H., and Gersten, K.: 2000, *Boundary-Layer Theory*, 8th Revised Edition, Springer-Verlag, Berlin, 799 pp. (See also Schlichting, *Boundary-Layer Theory*, McGraw-Hill, New York.)
11. Carminati, J., Devitt, J.S., and Scott, W.D.: 1995, On the non-uniqueness of solutions in the modelling of steady wind flows, *Comput. Fluids* **24**, 177–188.
12. Tennekes, H. and Lumley, J.L.: 1972, *A First Course in Turbulence*, MIT Press, Cambridge, MA, 300 pp.
13. Findlater, P.A. Carter, D.J. and Scott, W.D.: 1990, A model to predict the effects of prostrate ground cover on wind erosion, *Aust. J. Soil Res.* **28**, 609–622.
14. Brancatisano, A. and Trinh, D.T.: 1990, *Flow Conditions in a Wind Tunnel-Transition Section*, Bachelor of Engineering Project Report, Department of Mechanical Engineering, Curtin University of Technology, 139 pp. See also the Report from the Wind Erosion Study Group: 1992, *Erosion Wind Tunnel Workshop*, Environmental Science Report 92/8, ISBN No. 0-86905-448-1.
15. Raupach, M.R., Thom, A.S. and Edwards, I.: 1980, A wind tunnel study of turbulent flow close to regularly arrayed rough surfaces, *Boundary-Layer Meteorol.* **18**, 373–397.

16. Smith, S.E.: 1994, *An Instrument for Measuring Turbulence during Wind Erosion*, Ph.D. Thesis and Report 94/3, School of Environmental Science, Murdoch University, Perth, Western Australia.
17. Scott, W.D., Twomey, C., Butcher, L. and Kerr, J.: 1993, *The Murdoch Turbulence Probe* (19 min VHS Video), Academic Services Unit, Murdoch University, Perth, Western Australia.
18. Findlater, P.A.: 2004, *Using a Portable Wind Tunnel as a Tool to Predict Wind Erosivity*, Ph.D., School of Environmental Science, Murdoch University, Perth, Western Australia, Australia.
19. Raupach, M.R. and Leys, J.F.: 1990, Aerodynamics of a portable wind erosion tunnel for measuring soil erodibility by wind, *Aust. J. Soil Res.* **28**, 177–191.
20. Bagnold, R.A.: 1941, *Physics of Blown Sand and Desert Dunes*, Chapman and Hall, London 99 pp.
21. Lyons, T.J. and Scott, W.D.: 1990, *Principles of Air Pollution Meteorology*, CRC Press, Boca Raton, FL, 224 pp.
22. Scott, W.D.: 2001, *Maple for Environmental Sciences: A Helping Hand*, Section 5.6, Springer-Verlag, 395 pp.